

Active vibration control of a fluid/plate system using a pole placement controller

Bogdan Robu^{*}, Lucie Baudouin[†] and Christophe Prieur[‡]

March 10, 2011

Abstract

We consider the problem of active reduction of the structural vibrations induced by the sloshing of large masses of fuel inside a partly full tank. The proposed study focuses on an experimental device mimicking an aircraft wing made of an aluminum rectangular plate equipped with piezoelectric patches at the clamped end and with a cylindrical tip-tank, more or less filled with liquid. After deriving a representative finite dimensional model of the complete system, containing the first 5 structural modes of the plate and the first 3 liquid sloshing modes, a controller is computed. Since our main scope is to control the most energetic mode of the structure, a full state feedback method coupled with an observer is used. Finally, the controller is also tested for different initial conditions/perturbations and the results are compared with the ones obtained with an H_∞ controller. Experimental results illustrate the relevance of the chosen strategy.

^{*}Corresponding author. Email: brobu@laas.fr, CNRS; LAAS; 7 avenue du colonel Roche, F-31077 Toulouse, France. Université de Toulouse; UPS, INSA, INP, ISAE, UT1, UTM, LAAS; F-31077 Toulouse, France.

[†]CNRS; LAAS; 7 avenue du colonel Roche, F-31077 Toulouse, France. Université de Toulouse; UPS, INSA, INP, ISAE, UT1, UTM, LAAS; F-31077 Toulouse, France.

[‡]Department of Automatic Control, Gipsa-lab, Domaine universitaire, 961 rue de la Houille Blanche, BP 46, 38402 Grenoble Cedex, France,

Keywords

Flexible system, fluid/plate system, pole placement controller.

1 Introduction

As commercial transport aircraft designs become larger and more flexible, the impact of aeroelastic vibration of the flight dynamics increases in prominence. See e.g. [4], [19] or even [27] for airplanes and see [31] for helicopter dynamics. Moreover for space applications also, the interaction of flexible modes and sloshing modes disturbs the dynamics (see e.g. [3] or [10]).

For applications in aeronautics, it is crucial to suppress or to attenuate the plane wing's vibration when the wing is in interaction with the movement of the fuel inside of it (see e.g. [24]). Moreover, the movement of the fuel has critical impact on the stability of the plane (see [30] for example) and, coupled with the rigid body motion of the aircraft, it may create uncontrollable oscillations during flight which may even lead to the destruction of the engine (see [32]).

Smart materials are used for many applications e.g. in civil engineering. Thus flexible structures, which are equipped with piezoelectric patches, occupy a major place in the control research area. Their capability of attenuating the vibrations and measuring the deformation is described in [5], [6], [12] and [33] among other references. In the present paper it is shown that piezoelectric devices can be useful for vibration control in aeronautics for coupled fluid/flexible structure systems.

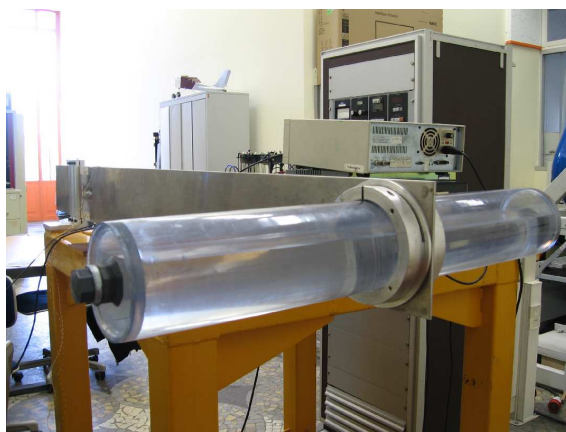


Figure 1: Plant description: the rectangular plate and the horizontal cylinder

In this objective, we study the experiment depicted by Figure 1 which is an example of a coupled fluid-flexible structure system. It has the same first flexible modes as a plane wing with fuel (see [26]). For vibration's attenuation of flexible structures, some studies investigate the use of piezoelectric patches to effectively suppress the vibrations (see [2], [9], [16], [35], [37], [38], [40] among others). However, only a few results are already available in the literature for fluid-structure systems. Reference [22] gives a recent theoretical result and [34] validates the method by means of experimental results. To the best of our knowledge, there are less studies of fluid-structure system dedicated to aerospace applications, except [25] where controllers are designed using a numerical model or our previous works [28] or [29], where an analytical model, described by approximated partial differential equations, is used.

In order to take into account the large number of degrees of freedom in the dynamics of the system, an infinite-dimensional model is first recalled in this paper. Afterwards, a truncation is performed in order to obtain a state-space model of the structure (see also [28]). Once the model is set, a controller is computed using the pole placement method (see for example [1], [14], [20], [39] among others). Although the method is well known in the literature, [23] can be checked for a feedback control implementation on a flexible structure. One advantage of this method, besides its simplicity of implementation, is that it gives the user the possibility to choose himself the location of the closed-loop system poles, therefore allowing the possibility of placing them at some predetermined locations. The main objective is the control of the most energetic mode of the structure (e.g. the plate vibrations along the first flexion mode). After the controller implementation, we check on experiments the relevance of the proposed control strategy.

The paper is organized as follows. We present in Section 2.1 the plant under consideration, equipped with piezoelectric patches (sensors and actuators). In Section 2.2 we give a brief presentation of the analytical model and we present the control objectives. Further on in Section 3, a controller is realized using the pole placement method and it's effectiveness is shown on experiments. Finally, in Section 4, a comparison between the pole placement and a H_∞ controller is discussed for other types of initial conditions and perturbations. Section 5 gives some concluding remarks.

2 Problem statement and control objectives

2.1 Plant description

The plant to be controlled is located at ISAE-ENSICA, Toulouse, France and has been constructed to have the vibration frequencies of a real plane wing filled with fuel in its tip-tank (see [26]).

The experimental device is composed of an aluminium rectangular plate and a plexiglas horizontal cylindrical tip-tank filled with liquid (see Figure 2).

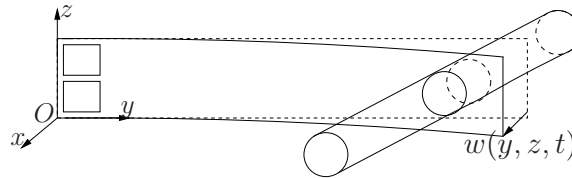


Figure 2: Deformation of the rectangular plate (1^{st} mode)

The length of the plate is along the horizontal axis and the width along the vertical one. The plate is clamped on one end and free on the three other sides. The characteristics of the aluminium plate are given in Table 1.

Plate length	L	1.36 m
Plate width	l	0.16 m
Plate thickness	h	0.005 m
Plate density	ρ	2970 kg m ⁻³
Plate Young modulus	Y	75 GPa
Plate Poisson coefficient	ν	0.33

Table 1: Plate characteristics

The two piezoelectric actuators made from PZT (Lead zirconate titanate) are bonded next to the plate clamped side. In order to create a moment, both actuators lengthen when a voltage is applied to their electrodes. Two sensors (made from PVDF - Polyvinylidene fluoride) are located on the opposite side of the plate with respect to the actuators. They will deliver a voltage proportional to their deformation. The characteristics of the collocated sensors and actuators are given in Table 2.

The tank is centered at 1.28 m from the plate clamped side and is symmetrically spread along the horizontal axis. Due to the configuration of the whole system (see Figure 2), the tank undergoes a longitudinal movement when the plate has a flexion

Actuator length/width/thickness	0.14/0.075/5e ⁻⁴ m
Sensor length/width/thickness	0.015/0.025/5e ⁻⁴ m
Actuator/Sensor density	7800 kg m ⁻³
Actuator/Sensor Young modulus	67 GPa
Actuator piezoelectric coefficient	-210e ⁻¹² m V ⁻¹
Sensor piezoelectric coefficient	-9.6 N (Vm) ⁻¹
Actuator/Sensor Poisson coefficient	0.3

Table 2: Characteristics of the piezoelectric patches

movement and a pitch movement if the plate has a torsion movement. It has the dimensions given in Table 3 and it can be filled with water or ice up to an arbitrary level. If the tank is filled with ice, it can be easily modeled by a steady mass (see [30]). When the tank is filled with water up to a level close to 0 or close to the cylinder diameter (near empty tank empty or near full tank), there is no sloshing behavior, and the modeling process is similar to the case of frozen water.

Tank exterior diameter	0.11 m
Tank interior diameter	0.105 m
Tank length	0.5 m
Tank density	1180 kg m ⁻³
Tank young modulus	4.5 GPa

Table 3: Characteristics of the cylindrical tank

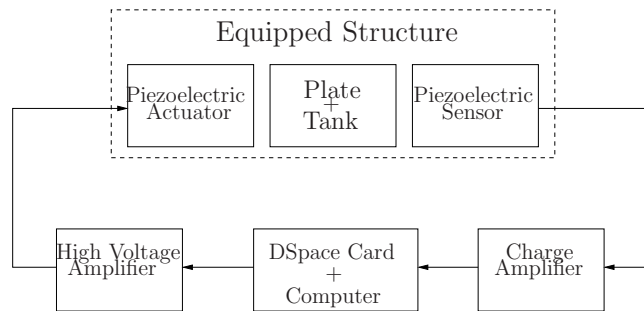


Figure 3: Equipped experimental setup

The experimental setup is depicted in Figure 3. The system (plate + tank) is

connected to the computer via a high voltage amplifier delivering ± 100 V and a charge amplifier 2635 from Brüer & Kjaer. Moreover, the controller is implemented in a DSpace© board.

First, the voltage delivered by the DSpace© card is amplified by the high voltage amplifier and then applied to the piezoelectric actuator. The deflection of the beam is measured by the piezoelectric sensor and then transmitted to the charge amplifier which will deliver a voltage to the DSpace© card. Concerning the acquisition chain, tests are made using a sampling time of 0.004 seconds on the DSpace© card.

2.2 Modeling and control objectives

For the controller implementation, the input of the system is the voltage applied to one of the piezoelectric actuators while the output of the system is the voltage measured with a piezoelectric sensor, collocated with the control actuator.

The mathematical model of the experimental device presented above was derived in our previous work (see [28]). Though the model is not detailed here, some general ideas are presented before the controller design.

Concerning the horizontal tank, it is known [17, Chapter 1] that the solution of the sloshing problem depends on the geometry of the tank. Since there are no analytical results for the mode frequencies, forces and moments of the dynamics in the horizontal cylindrical tank, a solution needs to be found.

As it was detailed in [28], we use a geometrical approximation in order to overcome this difficulty. The cylindrical tank is replaced by an “equivalent” rectangular one with the same sloshing frequencies (where length and width are respectively denoted a and b and are respectively along the x -axis and y -axis) and for which analytical results are available in the literature for the calculation of modes and forces/moments [17, Chapter 1.6].

On one hand, considering the plate, we derive the partial derivative equation of the plate (see [13, Chapter 4.6]):

$$m_s \frac{\partial^2 w}{\partial t^2} + \zeta(w) \frac{\partial w}{\partial t} + Y I_s \Delta^2 w = \frac{\partial^2 m_y}{\partial y^2} + \frac{\partial^2 m_z}{\partial z^2}$$

where $w = w(y, z, t)$ is the displacement, $\zeta(w)$ is an operator quantifying the damping, m_s mass per unit plate area, Y the Young modulus and $I_s = \frac{h^3}{12(1-\nu^2)}$ the moment of inertia of the plate. The Laplace operator is denoted Δ , with Δ^2 being equal to $\left(\frac{\partial^2}{\partial y^2} + \frac{\partial^2}{\partial z^2}\right)^2$ and m_y, m_z are external moments, along the y and z -axis, delivered to the plate by the actuators (see [11] or [8]) and by the sloshing modes of the liquid

in the tank. Furthermore the previous equation is to be solved using the boundary conditions given in [7, Chapter 8.1.1] for given initial conditions.

On the other hand, we now consider the longitudinal movement of the liquid along the x -axis. Since the liquid motion is starting from rest, there is a velocity potential $\phi(x, y, z, t)$ such that (see [21, Chapter 1.12]) the equation of liquid continuity is written as:

$$\frac{\partial^2 \phi}{\partial x^2} + \frac{\partial^2 \phi}{\partial y^2} + \frac{\partial^2 \phi}{\partial z^2} = 0.$$

The linearized (Bernoulli) equation of liquid motion is given by [21, Chapter 2.20] or [18]:

$$\frac{\partial \phi}{\partial t} + \frac{p}{\rho} + g(z - h) - C_0 x = 0$$

where C_0 stands for the acceleration along the x -axis, g for the gravitational acceleration and h for the liquid height in the container at rest position; ρ is the density of the liquid and $p = p(x, y, z, t)$ is the pressure in the liquid.

Moreover, the previous equations concerning the liquid motion are to be solved using the boundary conditions detailed in [21, Chapter 1.9] for the rectangular tank.

Concerning the coupling between these two equations, it is done by computing the influence of the plate on the liquid and vice-versa. More details about this issue are given in [28] or [29].

After a finite dimension approximation of the previous equations, we write the complete model of the structure as a state-space representation by considering only the first N modes for the plate and the first M liquid sloshing modes. Thus, the state space vector of the complete structure: $X = (X_p \ X_\theta)$ contains the state space vector of the plate X_p and the state space vector of the liquid X_θ :

$$\begin{cases} \dot{X} = \begin{pmatrix} A_p & A_{\theta p} \\ A_{p\theta} & A_\theta \end{pmatrix} X + \begin{pmatrix} B_p \\ B_{p\theta} \end{pmatrix} u \\ y = (C_p \ \mathbf{0}) X. \end{cases} \quad (1)$$

where $\begin{pmatrix} A_p & A_{\theta p} \\ A_{p\theta} & A_\theta \end{pmatrix} = A$ is the dynamic matrix of the structure, $\begin{pmatrix} B_p \\ B_{p\theta} \end{pmatrix} = B$ is the control matrix and $(C_p \ \mathbf{0}) = C$ is the output matrix with $\mathbf{0}$ denoting null matrices of appropriate dimensions.

As stated, the system model (1) is established for the first N modes of the plate and for the first M modes of the liquid sloshing. This is representative for the system behavior since it is shown in [15] that the first modes contain the main part of the energy of the deformation of the flexible structure. Moreover, using the energy approach from [36], it is possible to check that, in our particular case, the first 8 modes contain almost all the energy of the structure, with the first flexion mode of the plate containing around 65% of the total plate energy. Therefore, the controller will be computed for a system with $N = 5$ and $M = 3$. This implies $X_p \in \mathbb{R}^{10}$, $X_l \in \mathbb{R}^6$ and the total state space vector $X \in \mathbb{R}^{16}$.

The control objective is to attenuate the vibrations of the plate and the sloshing modes of the liquid in the tank for a plate initial deformation of 10cm realized at the plate free end. The deformation is along the first flexion mode of the plate, the most energetic mode. Finally, the results obtained are compared with the one given by a H_∞ control.

3 Controller synthesis

This section aims at computing a controller attenuating the plate vibrations along the first vibration mode. We are using here a state feedback strategy coupled with a Luenberger full state observer, since all the state-space vector of the system is unknown. Furthermore, based on the theory detailed in [14] or [39], we use a pole placement method in order to specify the closed-loop poles and the observer poles. Furthermore, the control scheme we are following is the one depicted in Figure 4, where the matrices to be determined are K and G of suitable dimensions.

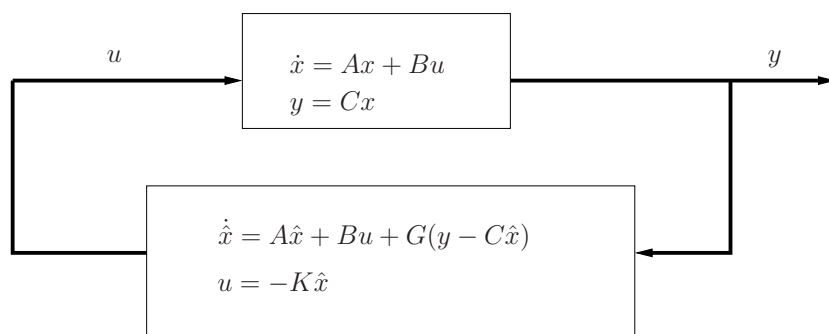


Figure 4: Feedback control law and observer

First, we compute the observability and controllability test matrices in order to be sure that all the system states are controllable and observable. Once this is set, we impose the dynamic of the state feedback law and of the observer. The poles which will specify the dynamic of the closed-loop system are chosen by selecting the poles of the $A - BK$ matrix while the ones for the observer dynamics are given by the poles of $A - GC$ matrix.

When choosing the poles one has to be very careful. In general the observer poles need to be faster than the closed-loop poles, since we want that the use of the observer does not decrease too much the performance with respect to the state feedback controller. We observed in practice that the fact of imposing very rapid poles for the observer leads to a noise amplification, thus a possible excitation of the high frequency system modes. Consequently, this will create a spillover effect, since the measurement noise is amplified. The same considerations are done for the closed-loop poles. Very fast closed-loop poles imply that: first, the voltage delivered by the controller might exceed the actuator limits of $\pm 100V$, thus possibly destabilizing the closed-loop system; second, the generated voltage might oscillate too fast in order to control the system. Thus, if the oscillating frequency is very high, the noise will be amplified, making the measurement impossible. One solution to this last issue is to select slower closed-loop poles but this will unavoidably lead to slower closed-loop response. We see therefore that a middle path needs to be found between the response time and the noise amplification.

By checking the open-loop system poles we find 8 complex conjugate poles (3 for the liquid sloshing and 5 for the plate), all of them having their real part negative. Thus the open-loop system is stable. The position of the open-loop poles can be seen in Figure 5, while their value is presented in Table 4 below.

Since the procedure for the controller synthesis is identical for all the tank filling levels, details are given here only for the case when the tank fill level e is 0.9. Let us first consider the choice of the pole placement controller K from Figure 4.

The choice of the closed-loop poles is very difficult. The best solution is to change only the real part of the dominant poles. In this case, the best closed-loop poles are given in Table 4. Concerning all the observer poles, their real part is three times bigger than the real part of the closed-loop poles.

The pole placement controller is tested on the experimental set-up for an initial plate displacement of 10cm at the free end. The controller response in attenuating the vibrations is presented in Figure 6, while the voltage delivered by the controller to make this attenuation is depicted in Figure 7.

It is important to notice that since the voltage delivered by the controller exceeds the maximum value of the voltage amplifier $\pm 100V$, the real voltage delivered to the

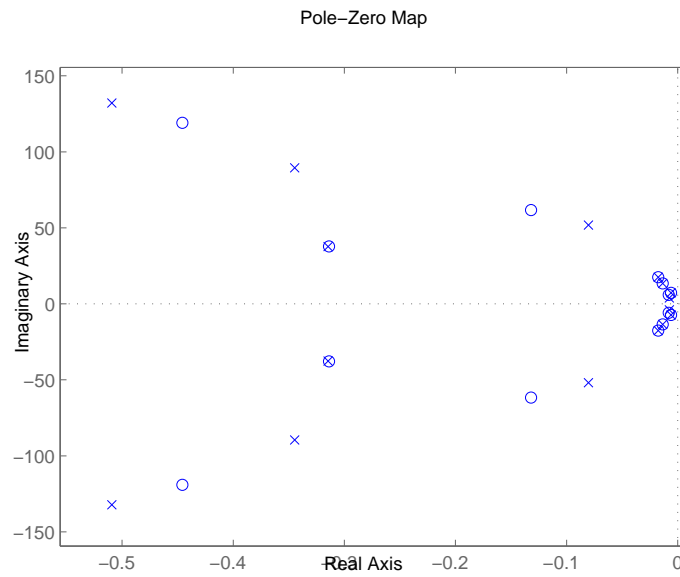


Figure 5: Pole/zero map of the open-loop system (\times for the poles, \circ for the zeros)

Open-loop poles	Closed-loop poles
$-0.5093 \pm 132.14i$	$-0.5093 \pm 132.14i$
$-0.3447 \pm 89.53i$	$-0.3447 \pm 89.53i$
$-0.0803 \pm 51.84i$	$-0.0803 \pm 51.84i$
$-0.3146 \pm 37.68i$	$-0.3146 \pm 37.68i$
$-0.0175 \pm 17.55i$	$-0.0325 \pm 17.55i$
$-0.0135 \pm 13.48i$	$-0.0384 \pm 13.48i$
$-0.0059 \pm 7.26i$	$-0.0333 \pm 7.26i$
$-0.0074 \pm 3.92i$	$-0.0324 \pm 3.92i$

Table 4: Closed-loop poles with the pole placement controller

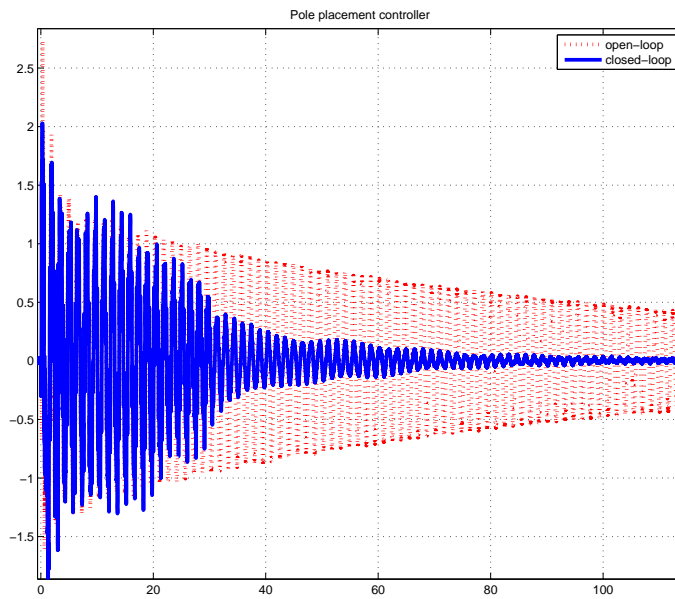


Figure 6: Experimental output of the of open-loop (dotted line) and closed-loop (plain line) systems using a pole placement controller with a tank fill level of 0.9

plate in the interval $0 \dots 30$ seconds is actually between -100V and $+100\text{V}$.

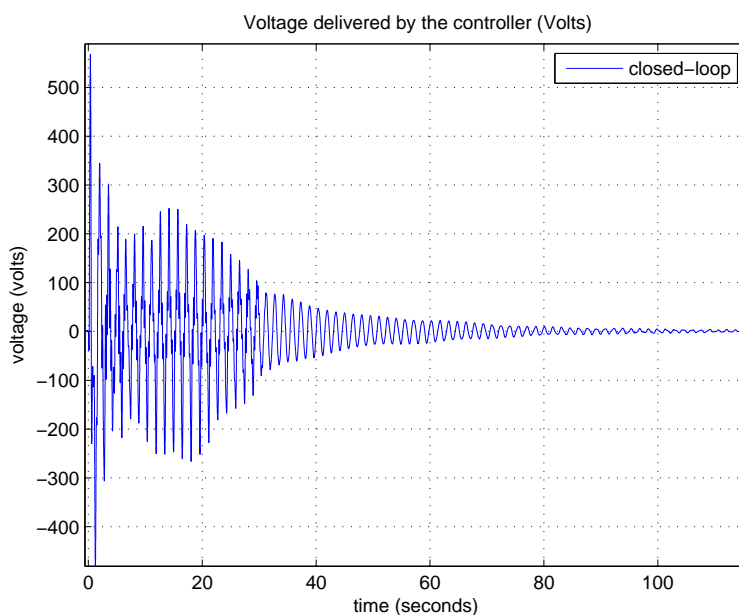


Figure 7: Voltage delivered by the pole placement controller during experiments

The frequency response of the system in closed-loop with the feedback controller previously computed is presented in Figure 8. We can notice that especially the first vibrations mode is well attenuated. Moreover, in a lower extent, the first sloshing mode (the second peak) experiences also some attenuation. We expected this to happen since the dominant poles, corresponding to the first mode of the plate and the first sloshing mode, are the ones that were mostly diminished. The other poles that were changed correspond to the other sloshing modes but their effect is not visible on the Bode plot due to their small amplitude of the concerned poles.

It is also interesting to notice that the second flexion mode also experiences a small attenuation, even though the corresponding poles have not been changed. This might be an influence of the other poles that have been shifted.

At the same time, we notice that the peaks corresponding to the torsion mode and to the other flexion modes have a larger amplitude. This means that testing the controller for a high frequency input would not give the best results since the controller is not computed to attenuate the large frequency values. Furthermore, in order to test this issue, we compare the previous results with the ones obtained using a control which has a wider action band.

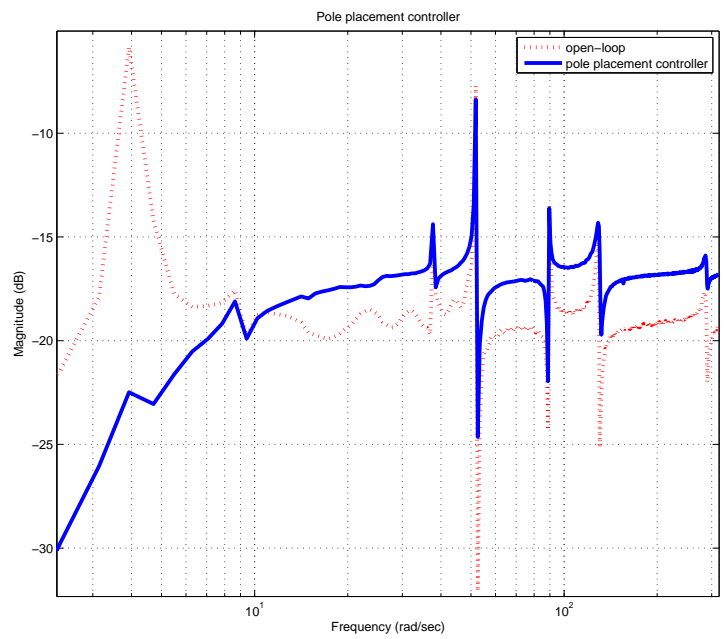


Figure 8: Frequency response of the pole placement controller

4 Other control types

Another type of control was implemented on this experimental device. One can check [29], where a H_∞ controller robust to external perturbations applied on the second piezoelectric actuator is computed and tested. The controller was calculated using the HIFOO library under Matlab.

In order to emphasize the advantages and the limitations of the controller calculated using the pole placement method, we compare the previous results to the ones obtained using the H_∞ controller from [29]. The results in temporal and frequency domains are presented below.

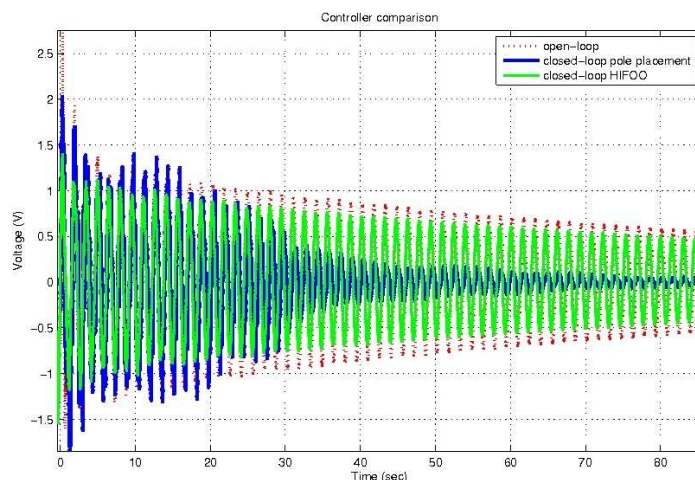


Figure 9: Temporal evolution of the experimental output for the closed-loop systems with pole placement controller (plain line) and H_∞ controller (bold line); plate free end deformation of 10cm

First of all, let us consider the case of the plate free end initial deformation of 10cm. The results are compared in Figure 9. As it can clearly be seen on experiments, the pole placement controller attenuates the plate oscillations much better than the controller computed using HIFOO does. Indeed, for the pole placement controller, the main modifications were made on the dominant poles, (see Table 4), that correspond to the first vibration and sloshing modes. Moreover, the robust controller from [29] was set to minimize the influence of the perturbations on the voltage generated by the controller. Thus, the voltage generated to control the plate movements is minimized for the H_∞ case while for the pole placement case is left

free. This is an explanation of the delivered voltage in both cases (around 500V for the pole placement controller and around 10V for the H_∞ one).

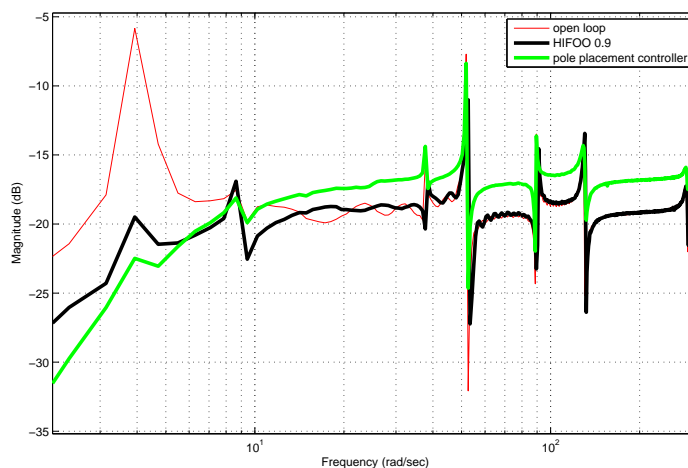


Figure 10: Experimental Bode plots for the closed-loop system with pole placement controller (plain line) and H_∞ controller (bold line)

Now, let us consider the Bode plots of the closed-loop systems in Figure 10. It can be easily seen that even though the pole placement controller attenuates more the first flexion mode, the H_∞ controller attenuates more the other high frequency modes and even attenuates the modes that were amplified by the former controller. In spite of these issues, when considering a wider frequency band the results given by the robust controller are better overall.

Finally, a discussion can be made concerning the controllers. The chosen control strategy depends strongly on the type of problem to be solved. If one knows that the structure will vibrate most of the time along the first flexion mode, then the pole placement controller is clearly the best choice. On the other hand, if we consider that the frequency range in which the plate vibrates is wide, we will prefer the H_∞ controller computed using HIFOO library from [29].

5 Conclusion

After describing the experimental device under consideration, some details were given concerning the computation of the analytical model. On a model with 5 vibration modes for the plate and 3 sloshing modes for the liquid in the tank, we proceeded

to the control of the structure. Using the pole placement method, we computed a controller that proves to be very effective when the plate is deformed along the first flexion mode. However, the results are less conclusive when considering a wider range of frequencies. In order to better quantify these results, some experiments are performed to compare with the ones obtained with a H_∞ controller from our previous work.

Acknowledgements

The authors would like to thank Valérie Pommier-Budinger, ISAE, Toulouse (France) for fruitful discussions on the experimental setup.

References

- [1] P.J. Antsaklis and A.N. Michel. *Linear systems*. Birkhäuser, 2006.
- [2] B.P. Baillargeon and S.S. Vel. Active vibration suppression of sandwich beams using piezoelectric shear actuators: Experiments and numerical simulations. *Journal of Intelligent Material Systems and Structures*, 16(6):517–530, 2005.
- [3] H. F. Bauer and K. Komatsu. Coupled frequencies of a frictionless liquid in a circular cylindrical tank with an elastic partial surface cover. *Journal of Sound and Vibrations*, 230(5):1147–1163, 2000.
- [4] J. Becker. Active buffeting vibration alleviation demonstration of intelligent aircraft structure for vibration & dynamic load alleviation. In *Proceedings of the US-Europe Workshop on Sensors and Smart Structures Technology*, pages 9–18, Commo and Soma Lombardo, Italy, April 2002.
- [5] J. Becker and W.G. Luber. Comparison of piezoelectric systems and aerodynamic systems for aircraft vibration alleviation. In *Smart Structures and Materials*, pages 9–18, San Diego, CA, March 1998.
- [6] B. Bhikkaji, S. O. R. Moheimani, and I. R. Petersen. Multivariable integral control of resonant structures. In *Proceedings of the 47th IEEE Conference on Decision and Control*, pages 3743–3748, Cancun, Mexico, December 2008.
- [7] R. D. Blevins. *Formulas for natural frequency and mode shape*. Krieger publishing company, Florida, 1995.

- [8] E. Crépeau and C. Prieur. Control of a clamped-free beam by a piezoelectric actuator. *ESAIM: Control, Optimization and Calculus of Variations*, 12:545–563, 2006.
- [9] K.K. Denoyer and M.K. Kwak. Dynamic modelling and vibration suppression of a swelling structure utilizing piezoelectric sensors and actuators. *Journal of Sound and Vibration*, 189(1):13–31, January 1996.
- [10] J.J. Deyst. Effects of structural flexibility on entry vehicle control systems. Technical Report NASA SP-8016, Nasa, Space Vehicle Design Criteria, April 1969.
- [11] E.K. Dimitriadis, C.R. Fuller, and C.A. Rogers. Piezoelectric actuators for distributed vibration excitation of thin plates. *Journal of Vibrational Acoustics*, 113:100–107, 1991.
- [12] A.J. Fleming and S.O. Reza Moheimani. Optimal impedance design for piezoelectric vibration control. In *Proceedings of the 43rd IEEE Conference on Decision and Control*, pages 2596–2601, Atlantis, Bahamas, December 2004.
- [13] M. Géradin and D. Rixen. *Mechanical Vibrations: theory and application to structural dynamics*. Masson, 1994.
- [14] G.C. Godwin, S.F. Graebe, and M.E. Salgado. *Control system design*. Prentice Hall, 2001.
- [15] D. Halim and S.O.R. Moheimani. An optimization approach to optimal placement of collocated piezoelectric actuators and sensors on a thin plate. *Mechatronics*, 13(1):27–47, February 2003.
- [16] J.K. Hwang, C.-H. Choi, C.K. Song, and J.M. Lee. Robust LQG control of an all-clamped thin plate with piezoelectric actuators/sensors. *IEEE/ASME Transactions on Mechatronics*, 2(3):205–212, September 1997.
- [17] R. A. Ibrahim. *Liquid sloshing dynamics*. Cambridge Univ. Press, 2005.
- [18] R.S. Khandelwal and N.C. Nigam. A mechanical model for liquid sloshing in a rectangular container. *Journal of the institution of engineers, India*, 69:152–156, 1989.
- [19] F. Kubica and C. Le Garrec. European patent office: "procédé et dispositif pour réduire les mouvements vibratoires d'un fuselage d'un aéronef". Technical report, Airbus France, May 2003.

- [20] B.C. Kuo. *Automatic control systems, second edition*. Prentice-Hall, N.J., 1967.
- [21] Sir H. Lamb. *Hydrodynamics*. Cambridge Mathematical Library, 1995.
- [22] I. Lasiecka and A. Tuffaha. Boundary feedback control in fluid-structure interactions. In *Proceedings of the 47th IEEE Conference on Decision and Control*, pages 203–208, Cancun, Mexico, December 2008.
- [23] F. Matsuno, T. Ohno, and Y.V. Orlov. Proportional derivative and strain (dps) boundary feedback control of a flexible space structure with a closed-loop chain mechanism. *Automatica*, 38(7):1201–1211, 2002.
- [24] K. F. Merten and B. H. Stephenson. Some dynamic effects of fuel motion in simplified model tip tanks on suddenly excited bending oscillations. Technical report, Langley Aeronautical Laboratory, Langley Field, Va., 1952.
- [25] V. Pommier-Budinger, Y. Janat, D. Nelson-Gruel, P. Lanusse, and A. Oustaloup. Fractional robust control with iso-damping property. In *Proceedings of the 2008 American Control Conference*, pages 4954–4959, Seattle, WA, June 2008.
- [26] V. Pommier-Budinger, J. Richelot, and J. Bordeneuve-Guibé. Active control of a structure with sloshing phenomena. In *Proceedings of the IFAC Conference on Mechatronic Systems*, Heidelberg, Germany, 2006.
- [27] D.L. Raney, E. B. Jackson, C. S. Buttrill, and W. M. Adams. The impact of structural vibration on flying qualities of a supersonic transport. In *AIAA Atmospheric Flight Mechanics Conference*, Montreal, Canada, 2001.
- [28] B. Robu, L. Baudouin, and C. Prieur. A controlled distributed parameter model for a fluid-flexible structure system: numerical simulations and experiment validations. In *Proceedings of the 48th IEEE Conference on Decision and Control and 28th Chinese Control Conference*, pages 5532–5537, Shanghai, P.R. China, December 2009.
- [29] B. Robu, V. Budinger, L. Baudouin, C. Prieur, and D. Arzelier. Simultaneous H_∞ vibration control of a fluid/plate system via reduced-order controller. In *Proceedings of the 49th IEEE Conference on Decision and Control*, pages 3146–3151, Atlanta, GE. USA, December 2010.

- [30] J.-S. Schotte and R. Ohayon. Various modelling levels to represent internal liquid behavior in the vibration analysis of complex structures. *Journal of Computer Methods in Applied Mechanics and Engineering*, 198:1913–1925, 2009.
- [31] J. Shaw and N. Albion. Active control of the helicopter rotor for vibration reduction. *Journal American Helicopter Society* 26, 26:32–40, July 1981.
- [32] R. F. Stengel. *Flight Dynamics*. Princeton University Press, Princeton and Oxford, 2004.
- [33] H. Sun, Z. Yang, KX. Li, B. Li, J. Xie, D. Wu, and LL. Zhang. Vibration suppression of a hard disk driver actuator arm using piezoelectric shunt damping with a topology-optimized PZT transducer. *Journal of Smart Materials and Structures*, 18:1–13, 2009.
- [34] T. Terasawa, C. Sakai, H. Ohmori, and A. Sano. Adaptive identification of MR damper for vibration control. In *Proceedings of the 43rd IEEE Conference on Decision and Control*, pages 2297–2303, Atlantis, Bahamas, December 2004.
- [35] S. Tliba. h_2 controller design for active vibration damping: experimental results. In *Proceedings of the 5th IFAC Symposium on Robust Control Design*, Toulouse, France, July 5-7 2006.
- [36] S. Tliba and H. Abou-Kandil. H_∞ control design for active vibration damping of flexible structure using piezoelectric transducers. In *Proceedings of the 4th IFAC Symposium on Robust Control Design*, Milan, Italy, June 2003.
- [37] S. Tliba, H. Abou-Kandil, and C. Prieur. Active vibration damping of a smart flexible structure using piezoelectric transducers: H_∞ design and experimental results. In *Proceedings of the 16th IFAC World Congress*, Praha, Czech Republic, July 2005.
- [38] K. Yamada, H. Matsuhisa, and H. Utsuno. Hybrid vibration suppression of multiple vibration modes of flexible structures using piezoelectric elements and analog circuit. In *Proceedings of World Forum on Smart Materials and Smart Structures Technology*, pages 317–318, P. R. China, May 2007.
- [39] L.A. Zadeh and C.A. Desoer. *Linear system theory, the state space approach*. McGraw Hill Book Company, New York, 1963.

- [40] J. Zhang, L. He, E. Wang, and R. Gao. Active vibration control of flexible structures using piezoelectric materials. In *Proceedings of the 2009 International Conference on Advanced Computer Control*, pages 540–545, Shenyang, P.R. China, January 2009.